Journal of Drug Delivery Science and Technology 60 (2020) 101964

Contents lists available at ScienceDirect

Journal of Drug Delivery Science and Technology

journal homepage: www.elsevier.com/locate/jddst

Research paper

Controlled delivery of ketamine from reduced graphene oxide hydrogel for neuropathic pain: *In vitro* and *in vivo* studies

Rui Wang [a], Jianhui Gan [b,1], Renhu Li [c,1], Jinghui Duan [a], Jianjun Zhou [d], Miaomiao Lv [e], Rongqin Qi [f,*]

[a] Department of Anesthesiology, HanDan Cetral Hospital, HanDan, Hebei, 063000, China
[b] Department of Anesthesiology, The Affliated Tangshan People Hospital of North China University of Science and Technology, Tangshan, Hebei, 063000, China
[c] Department of Anesthesiology, The Luan Affiliated Hospital of Anhui Medical University, Luan, Anhui, 237005, China
[d] Department of Anesthesiology, Jiangsu Danyang Traditional Chinese Medicine Hospital, Danyang City, Jiangsu Province, 212309, China
[e] Department of Anesthesiology, The 323 Hospital of PLA, Xi'an, Shaanxi, 713600, China
[f] Department of Anesthesiology, Jinan Maternity and Child Care Hospital, Jinan, Shandong, 250001, China

ARTICLE INFO

Keywords:
Ketamine
Reduced graphene oxide
Pluronic® F127
Transdermal
Sustained release
Animal studies

ABSTRACT

Ketamine which is widely used to manage neuropathic pain shows major limitations of low oral bioavailability (10–20%) and short half-life (<2 h), which affects the routine life style of patients (noncompliance due to multiple dosing and associated side effects). The current research aim to developed ketamine loaded Pluronic® F127 stabilized reduced graphene oxide hydrogel for sustain drug delivery via transdermal route. The Fourier transform infrared spectroscopy, Raman spectroscopy, and X-ray diffraction data confirm the attachment of Pluronic® F127 on the reduced graphene oxide. The scanning electron microscopy image showed the wrinkled and flattened nano-sheet surface with the presence of micelles. The *ex vivo* flux decreases proportionally with increase in the level of graphene oxide, which suggests that the ketamine release rate can be the tailored by changing the level of graphene oxide in the hydrogel. The writing test in mice confirmed low analgesic activity of ketamine loaded reduced graphene oxide hydrogel due to low flux rate of drug in comparison to control ketamine hydrogel (without graphene oxide). The tail-flick study on Wistar rats showed prolonged analgesic effect (24 h) with ketamine loaded reduced graphene oxide in comparison to ketamine control hydrogel (4 h). Thus, ketamine loaded Pluronic® F127-reduced graphene oxide hydrogel can be used to manage the neuropathic pain for the extended period of time bypassing associated side effects of intravenous, nasal and oral routes.

1. Introduction

Neuropathic pain defined by the International Association for the study of Pain (IASP) is because of primary lesion or dysfunction of the nervous system [1,2]. Neuropathic pain a possible outcome of many central and peripheral nerve disorders increases with aging of population [3–5]. The clinical features include allodynia, numbness, hyperalgesia, weakness, burning, and shooting [6–9]. The development of effective therapy to treat neuropathic pain is in its infancy [10,11]. The first line treatment includes the use of tricyclic antidepressants, pregabalin, topical lidocaine, opioid analgesics, antiepileptic, etc. [12–14]. However, the oral medications have been limited due to systemic side effects [15,16].

Ketamine is a non-competitive N-methyl-D-aspartate (NMDA) receptor antagonist used as anaesthetic, sedative, analgesic and for the management of neuropathic pain [17]. Intravenous route of ketamine administration is expensive (short half-life < 2 h), inconvenient, and associated with systemic side effects with increase in the risk of addiction [18,19]. Intra nasal route may increase the risk of irritation and nasal epithelium damage [19]. Oral route is inconvenient due to short half-life and low oral bioavailability (10–20%) due to high first pass metabolism (19 ml/min/kg) [18,20]. The issue can be addressed by transdermal route via hydrogel system [21–25], which could also maintain the required therapeutic ketamine concentration by tailoring the amount of Pluronic® F127 stabilized reduced graphene oxide in the hydrogel system.

* Corresponding author.
E-mail address: qll64931254@sina.com (R. Qi).
[1] This authors have equal contribution.

https://doi.org/10.1016/j.jddst.2020.101964
Received 20 April 2020; Received in revised form 28 June 2020; Accepted 21 July 2020
Available online 2 August 2020

In the present work, Pluronic® F127 stabilized reduced graphene oxide was used to tailor the release rate of ketamine from the hydrogel prepared using Carbopol 940. The π- π stacking interaction between the ketamine and the reduced graphene oxide control the release of ketamine from the hydrogel system [26–28]. Maryam and co-workers used dopamine functionalized graphene oxide to deliver cytarabine [29]. Florina and co-workers used graphene oxide for photo-thermal permeation of ondansetron to improve skin permeation [30]. Duygu and co-workers used reduced graphene oxide reinforced hyaluronic acid/-gelatin/poly(ethylene oxide) film to module the release of irbesartan [31]. Ali and co-workers developed novel oxygen rich functionalized graphene oxide as a pH sensitive polymer to deliver curcumin and doxorubicin, with improved cellular uptake for cancer treatment [32]. Hassan and co-workers used graphene oxide to deliver doxorubicin and paclitaxel [33]. Several approaches have been developed to improve the permeation of drug across the skin layers. Zapantis and co-workers studied the systemic absorption of ketamine and noted better absorption of hydrogel in comparison to ketamine cream [34]. August and co-workers noted better percutaneous absorption of ketamine HCl with peak level at 6 h [35]. Mingsheng and co-workers prepared transdermal hydrogel of ketamine using chitosan and Poloxamer 407 and observed prolong analgesia [36]. Rie and co-workers developed ketamine transdermal patch and noted 50 ng/ml plasma concentration [37]. Basant and co-workers demonstrate the use of vesicular system to improve the permeation of drug across the skin layers [38]. Raid and co-workers used microemulsion to increase the permeation of ondansetron via transdermal route [39]. The aim of the study was to formulate the ketamine loaded Pluronic® F127-reduced graphene oxide hydrogel to sustain the release of ketamine for prolong therapeutic effect to manage neuropathic pain. The in-depth *in vitro* and *in vivo* studies were performed to understand the potential of the developed ketamine loaded Pluronic® F127-reduced graphene oxide hydrogel.

2. Materials and methods

2.1. Materials

Ketamine was supplied by Jiangsu Hengrui Medicine Company Limited (Jiangsu Province, China). Graphite, Pluronic® F127, Carbopol and other required chemicals were purchased from Sigma Aldrich Chemicals (MO, USA). Deionized water was produced from Millipore-Q purification system.

2.2. Synthesis of Pluronic® F127 stabilized reduced graphene oxide (P-rGO)

Graphene oxide (GO) was synthesized by modified Hummer's method from graphite using potassium permanganate and sulphuric acid [40,41]. Reduced graphene oxide (rGO) was synthesized from GO using ascorbic acid [42]. Pluronic® F127 stabilized reduced graphene oxide (P-rGO) was synthesized in a similar way by adding 800 mg of Pluronic® F127 in 15 ml of GO solution (1 mg/ml). The ascorbic acid (2 mM) was added in the above solution and stirred vigorously for 3 h at 90 °C. The GO solution (brown color) was reduced to black P-rGO (reduced graphene oxide) aggregates by ascorbic acid. The aggregates were washed several times using water and dried.

2.3. Characterization of Pluronic® F127 stabilized reduced graphene oxide (P-rGO)

The size (hydrodynamic) and polydispersibility index (PDI) of GO, rGO, and P-rGO was investigated by dynamic light scattering (DLS) at 25 °C using Zetasizer Nano ZS (90° incident angle) by Malvern Instrument (USA) [43–45]. The fourier transform infrared spectroscopy (FTIR) spectroscopy was used to investigate the reduction efficacy of GO to rGO and P-rGO [46,47]. The spectra were recorded using FTIR-Bruker Alpha-E model (Perkin, USA) in the region of 4000–500 cm^{-1}. Raman spectroscopy (STR 300, Airix Corporation, Japan) was performed to investigate the electrical and structural properties of the graphite, GO, rGO and P-rGO [48–50]. X-ray diffraction (XRD) study was performed using Analytical X'pert Pro MRD (Netherland) to assess the crystalline property of the graphite, GO, rGO and P-rGO [51]. The scanning electron microscopy (TEM) was performed to study the morphology of rGO and P-rGO using Zeiss scanning electron microscopy (Carl Zeiss, New York) [52–54].

2.4. Ketamine loaded transdermal hydrogel

Ketamine (5% w/w) was added in the P-rGO dispersion at varying concentration (0.1 μg/ml, 1 μg/ml and 10 μg/ml coded as K–P-rGO-0.1-Gel, K–P-rGO-1-Gel and K–P-rGO-10-Gel) and kept under mild stirring for 24 h. The viscosity of the ketamine loaded P-rGO dispersion was increased by adding 2% Carbopol 940 (overnight hydration) for topical application [55]. Control batch was also prepared without P-rGO dispersion (K-Gel).

2.5. Viscosity and pH of hydrogel

The viscosity of ketamine loaded P-rGO hydrogels were determined by Brookfield DV-III Rheometer using SC4-18 spindle (Brookfield Engineering Laboratory, USA) [45]. The pH was determined by digital pH meter at room temperature. The study was carried out in triplicate.

2.6. Ex vivo drug release study

The *ex vivo* ketamine release study was conducted on K-Gel, K–P-rGO-0.1-Gel, K–P-rGO-1-Gel and K–P-rGO-10-Gel hydrogels using goat skin and modified Franz diffusion cell (1.0 cm^2 diffusion area) [56–58]. The skin was supplied from the local slaughter house and hairs were removed using depilator. The receiver compartment was filled with 15 ml of phosphate buffer saline solution (37 °C, pH 7.4) and the donor compartment was filled with 0.2 gm of hydrogel (equivalent to 10 mg of ketamine) under occlusive conditions. At regular time intervals, the sample (aliquot) was collected from the receiver compartment and same volume was replaced with the fresh media. The amount of ketamine was quantified using HPLC at 215 nm [59,60]. The study was carried out in triplicate.

2.7. Animal studies

The rabbits and Wister rats were approved HanDan Certral Hospital, China (20190324000A).

2.7.1. Skin irritation study

The skin irritation study was performed to investigate the side effects like discomfort, erythaema and oedema [61,62]. The rabbits were divided into two groups (n = 3) and 2 × 2 cm^2 area of dorsal skin was denuded using razor and cleaned with alcohol. Two hours after denuded using razor, the K–P-rGO-1-Gel hydrogel (5 %w/w) and control hydrogel (K-Gel, 5 %w/w) was applied on the rabbit skin area. At regular time intervals the area (application site) was scored for erythaema and oedema (7 days).

2.7.2. Writhing test

The writhing test was conducted using male Swiss albino mice (25–30 gm) to assess the analgesic activity of K–P-rGO-1-Gel hydrogel (5 %w/w) and control hydrogel (K-Gel, 5 %w/w); and compared with topical 5 %w/w marketed lidocaine ointment (n = 6). After 3 h of topical application, the writing was induced in mice by intraperitoneal injection of 1% v/v acetic acid solution (10 ml/kg) [63,64]. The number of writhes was recorded for 15 min and the analgesic activity was evaluated in terms of the percentage of writhe inhibitions using following

equation.

$$\% \text{ Inhibition} = \frac{\text{Average writhes in control group} - \text{Average writhes in test group}}{\text{Average writhes in control group}} \times 100$$

2.7.3. Radiant heat tail flick test

The radiant heat tail flick study was performed to investigate the efficacy of K–P-rGO-1-Gel hydrogel (5 %w/w) and control hydrogel (K-Gel, 5 %w/w); and compared with topical 5 %w/w marketed lidocaine ointment (n = 6). The efficacy test was performed on male Wistar rats (three group, n = 6) using analgesiometer (Beijing Channel Scientific Co. Ltd, Beijing, China) [65–67]. The formulation was applied on the root (midline) of the rat tail and the reaction time was monitored at pre-determined time intervals by exposing to analgesiometer at 55 °C. The cut off basal reaction time was fixed at 10 s. The analgesic effect was determined using following formula.

$$\% \text{ Anaesthetic effect} = \frac{\text{observed reaction time} - \text{basal reaction time}}{\text{cut} - \text{off time period} - \text{basal reaction time}} \times 100$$

3. Results and discussion

3.1. Characterization of Pluronic® F127 stabilized reduced graphene oxide

Characterization was performed to investigate the formation of rGO from GO and the attachment of Pluronic® F127 on rGO. The DLS reports are shown in supplementary material part A. The hydrodynamic size of GO, rGO and P-rGO was found to be 942 nm (PDI = 0.212), 1123 nm (PDI = 0.143) and 823 nm (PDI = 0.111). Thus, the presence of Pluronic® F127 stabilized the P-rGO with better PDI value.

The FTIR reports are shown in Fig. 1 (A). The GO shows characteristic stretching vibration of epoxy group (C–O stretching) at 1060 cm^{-1}, C–OH stretching at 1217 cm^{-1}, C═O at 1720 cm^{-1}, O–H stretching at 3550 cm^{-1}, skeletal vibration of sp^2 at 1620 cm^{-1} and tetrahedral stretching at 2949 cm^{-1} which suggest the presence of –CH group in GO. The r-GO spectra shows reduction in the intensity of characteristic peaks [stretching vibration (C═O) at 1730 cm^{-1} and C–OH stretching at 1217 cm^{-1}] and the absence of epoxy peak, which indicate reduction of GO to rGO. The FTIR spectra of Pluronicμ® F127 shows characteristic peak at 1109 cm^{-1} (C–O–C stretching), 2879 cm^{-1} (C–H stretching), and 3450 cm^{-1} (O–H stretching). The FTIR spectra of P-rGO shows all characteristic peaks of Pluronic® F127 along with the characteristic peaks at 3450 cm^{-1} (O–H stretching), which suggest the functionalization of Pluronic® F127 on rGO.

The Raman spectra are shown in Fig. 1 (B). The graphite shows 1330 cm^{-1} (D band), 1558^{-1} (G band) and 2683^{-1} (2D band) characteristic peaks. The prominent G band was observed in all Raman spectra due to phonon scattering of graphitic structure (in plane vibrational mode of sp^2 hybridized carbon atoms). The D band represents a ring breathing mode from sp^2 carbon atoms which are adjacent to the edge (defect site) in the graphitic plane. The graphite (highly ordered) shows strong peak at G band and weak peak at D band. The D band peak was prominent in GO and rGO structure, indicating significant structural disorder due to oxidation.

The XRD patterns are shown in Fig. 1 (D). The characteristic peak of graphite, GO and rGO was noted at 26.5°, 11.2°, and 26.5° respectively, which corresponds to d-spacing values of 3.36 Å, 8.32 Å, and 8.21 Å respectively. The P-rGO shows its characteristic peak at 23.24 Å (d-

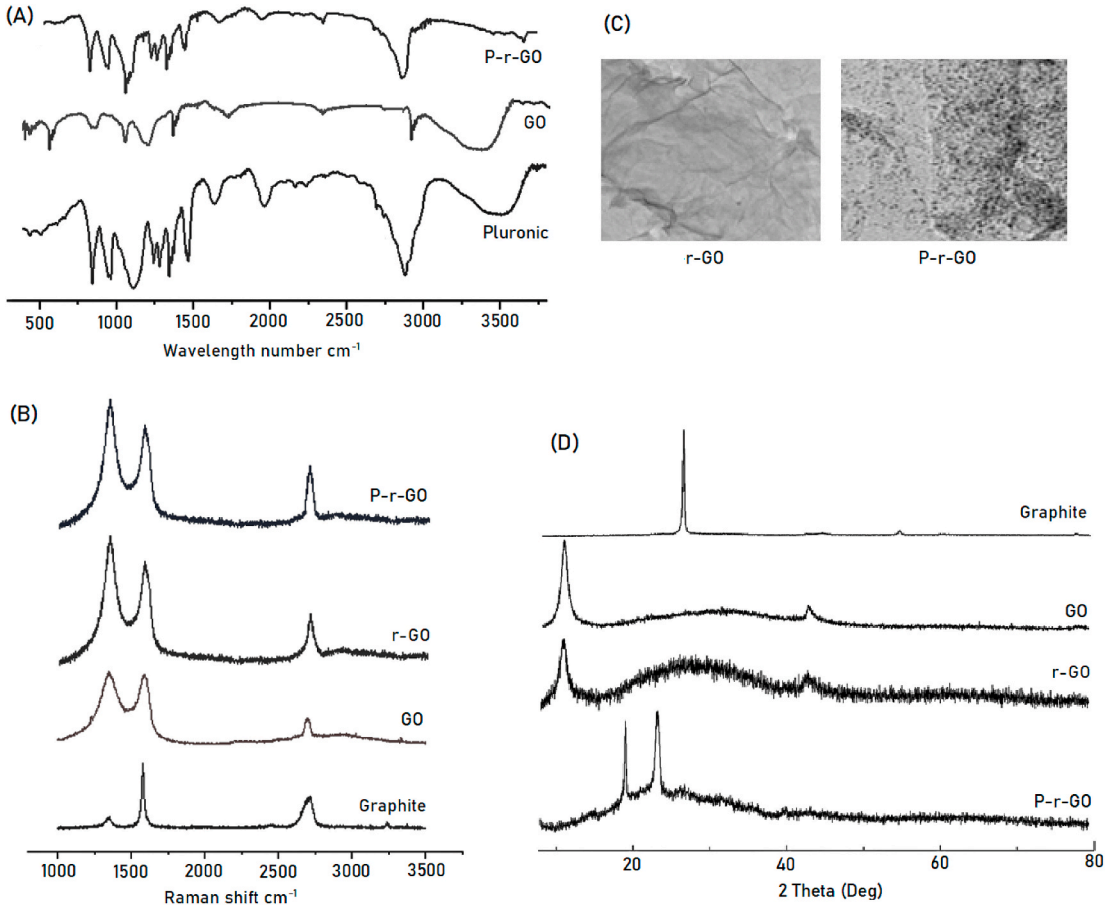

Fig. 1. (A) FTIR reports, (B) Raman spectra, (C) SEM images, and (D) XRD patterns.

spacing = 4.66 Å). The SEM image of rGO show wrinkled and thick flattened nano-sheet surface, which was due to organic and electrostatic interaction of oxides [Fig. 1 (C)]. The P-rGO shows the presence of Pluronic® F127 micelles on the surface, which was expected.

3.2. Viscosity and pH of hydrogel

Viscosity of K-Gel, K–P-rGO-0.1-Gel, K–P-rGO-1-Gel and K–P-rGO-10-Gel hydrogels at 100 rpm was found to be 16,133, 16,767, 16,866 and 16,988 cp respectively. The viscosity was sufficient for smooth application and retention of hydrogel on the skin surface for transdermal application. The pH of O-Gel, K–P-rGO-0.1-Gel, K–P-rGO-1-Gel and K–P-rGO-10-Gel hydrogels was found to be 5.51 ± 0.12, 5.52 ± 0.21, 5.45 ± 0.11 and 5.34 ± 0.21 respectively, which fall in the normal range of skin pH (4–6). Thus, the gel would not irritate the skin upon local application [68].

3.3. Ex vivo drug release study

Ex vivo drug release study was performed to evaluate the release of ketamine from the hydrogels and to study the effect of reduced graphene oxide on the release profile of ketamine. The *ex vivo* drug release graphs are shown in Fig. 2. The control K-Gel hydrogel (without P-rGO) showed highest release of ketamine from the hydrogel system [flux (J) = 380.6 μg/cm^2/h). The high flux rate was due to absence of any controlling system in the hydrogel except the viscosity of the gelling system due to Carbopol. In contrast, the flux (J) of K–P-rGO-0.1-Gel, K–P-rGO-1-Gel and K–P-rGO-10-Gel hydrogels were significantly decreased ($p < 0.01$), it was found to be 120.0, 70.5, and 42.2 μg/cm^2/h respectively. The low flux value indicate that the release of ketamine from the Pluronic® F127 stabilized reduced graphene oxide was slow due to π- π stacking interaction between the drug and graphene oxide [69,70]. The flux decreases proportionally with increase in the level of graphene oxide, which suggests that the drug release rate can be the tailored by changing the level of graphene oxide in the system. We have selected K–P-rGO-1-Gel batch for further *in vivo* studies, as it showed sufficient flux for therapeutic response [71,72].

3.4. Skin irritation study

The skin irritation study was performed on rabbit skin to investigate the side effects like discomfort, erythaema or oedema. No skin irritation was observed during 7 days of treatment period with both the hydrogels [control gel (K-Gel) and ketamine (K–P-rGO-1-Gel)].

3.5. Writhing test in mice

The analgesic activity of selected K–P-rGO-1-Gel batch was evaluated based on the ability of the gel to inhibit the pain in the mice induced by challenging i. p. injection of 1% acetic acid. The percentage inhibition (writhes) by standard marketed lidocaine ointment and ketamine control gel (K-Gel) was found to be 65.7 ± 5.1% and 58.4 ± 5.8% respectively. While, percentage inhibition of K–P-rGO-1-Gel batch was 49.7 ± 6.8%, the low percentage inhibition of writhes was due to low flux value of ketamine in the presence of reduced graphene oxide in comparison to control ketamine hydrogel (K-Gel). Thus, to achieve the optimum level of therapeutic effect (release rate profile), further tailoring of the amount of reduced graphene oxide is mandatory.

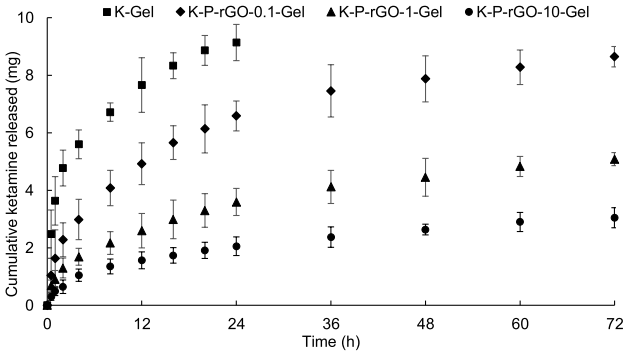

Fig. 2. *Ex vivo* ketamine diffusion across the goat skin from the control hydrogel (G–O) and ketamine loaded Pluronic® F127 stabilized reduced graphene oxide hydrogels (n = 3, mean ± standard deviation).

3.6. Radiant heat tail flick test

The basal reaction time (control group) in the radiant heat tail-flick method was found to be 2.44 s (Fig. 3). The marketed lidocaine ointment showed maximum response of 6.59 s at 2 h, which falls rapidly due to high clearance rate of ointment. The ketamine control hydrogel (K-Gel) showed peak effect at 2 h (6.51 s), followed by prolonged analgesic effect for 4 h. While, K–P-rGO-1-Gel hydrogel showed peak effect at 8 h (5.72 s), the analgesic effect was extended for 24 h. The extended analgesic effect was due to sustain release of ketamine from the Pluronic® F127 stabilized reduced graphene oxide. However, initial burst release and optimization is needed to achieve the desired initial concentration for quick analgesic effect. Allover, significant ($p < 0.01$) improvement in the extension of analgesic effect was noted with ketamine loaded reduced graphene oxide in comparison to ketamine control hydrogel.

4. Conclusion

The research work successfully demonstrate the application of Pluronic® F127 stabilized reduced graphene oxide to sustain the release of ketamine due to unique π- π stacking interaction between ketamine and reduced graphene oxide. The Raman spectroscopy, FTIR, and X-ray diffraction data confirmed the attachment of Pluronic® F127 on the reduced graphene oxide. The TEM image showed the wrinkled and flattened nano-sheet surface with the presence of Pluronic F127 micelles. The *ex vivo* release study showed sustained release of ketamine from the Pluronic® F127 stabilized reduced graphene oxide hydrogel (2% Carbopol 940 base) in comparison to the control hydrogel (without reduced graphene oxide). The flux decreases proportionally with increase in the level of graphene oxide, which suggests that the ketamine release rate can be the tailored by changing the level of graphene oxide in the hydrogel. No irritation was noted on the rabbit's skin study. The writing study in the mice showed relatively low analgesic activity of selected K–P-rGO-1-Gel batch due to low flux rate of ketamine in the presence of reduced graphene oxide in comparison to control ketamine

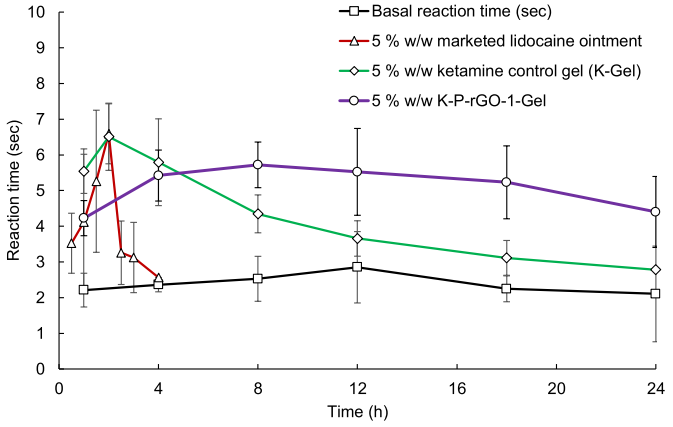

Fig. 3. Reaction time in radiant heat tail flick study in male Wistar rats (mean ± standard deviation, n = 6).

hydrogel (K-Gel). The radiant heat tail-flick study showed prolonged analgesic effect with ketamine loaded reduced graphene oxide in comparison to ketamine control hydrogel. Thus, ketamine loaded Pluronic® F127-reduced graphene oxide hydrogel can be used to manage the neuropathic pain for the extended period of time bypassing associated side effects of intravenous, nasal and oral routes. The Pluronic® F127 stabilized reduced graphene oxide hydrogel can also be used for other hydrophobic drugs for sustain release to treat topical diseases.

CRediT authorship contribution statement

Rui Wang: Investigation, Methodology, Validation, Writing - original draft. **Jianhui Gan:** Formal analysis, Data curation, Visualization. **Renhu Li:** Formal analysis, Data curation, Visualization. **Jinghui Duan:** Project administration, Writing - review & editing. **Jianjun Zhou:** Software. **Miaomiao Lv:** Resources, Supervision. **Rongqin Qi:** Conceptualization, Funding acquisition.

Declaration of competing interest

There are no known conflicts of interest associated with this publication and there has been no significant financial support for this work that could have influenced its outcome.

Appendix A. Supplementary data

Supplementary data to this article can be found online at https://doi.org/10.1016/j.jddst.2020.101964.

References

[1] M.-M. Backonja, Defining neuropathic pain, Anesth. Analg. 97 (3) (2003) 785–790.
[2] C.J. Vecht, Nociceptive nerve pain and neuropathic pain, Pain Med. 39 (2) (1989) 243–244.
[3] K. Meacham, A. Shepherd, D.P. Mohapatra, S. Haroutounian, Neuropathic pain: central vs. peripheral mechanisms, Curr. Pain Headache Rep. 21 (6) (2017) 28–35.
[4] C.J. Woolf, The pathophysiology of peripheral neuropathic pain—abnormal peripheral input and abnormal central processing, Advances in Stereotactic and Functional Neurosurgery 10 (1993) 125–130. Springer.
[5] C.J. Woolf, R.J. Mannion, Neuropathic pain: aetiology, symptoms, mechanisms, and management, Lancet 353 (9168) (1999) 1959–1964.
[6] C. Fear, Neuropathic pain: clinical features, assessment and treatment, Nurs. Stand. 25 (6) (2010) 1–10.
[7] H. Klit, N.B. Finnerup, T.S. Jensen, Central post-stroke pain: clinical characteristics, pathophysiology, and management, Lancet Neurol. 8 (9) (2009) 857–868.
[8] R. Benoliel, Y. Zadik, E. Eliav, Y. Sharav, Peripheral painful traumatic trigeminal neuropathy: clinical features in 91 cases and proposal of novel diagnostic criteria, J. Orofac. Pain 26 (1) (2012) 1–10.
[9] J. Scadding, M. Koltzenburg, Neuropathic pain, Adv Clin Neurosci Rehabil 3 (2) (2003) 8–14.
[10] M. Delforge, J. Bladé, M.A. Dimopoulos, T. Facon, M. Kropff, H. Ludwig, A. Palumbo, P. Van Damme, J.F. San-Miguel, P. Sonneveld, Treatment-related peripheral neuropathy in multiple myeloma: the challenge continues, Lancet Oncol. 11 (11) (2010) 1086–1095.
[11] D. Ziegler, Treatment of diabetic neuropathy and neuropathic pain: how far have we come? Diabetes Care 31 (2008) S255.
[12] A.B. O'Connor, R.H. Dworkin, Treatment of neuropathic pain: an overview of recent guidelines, Am. J. Med. 122 (10) (2009) S22–S32.
[13] R.H. Dworkin, M. Backonja, M.C. Rowbotham, R.R. Allen, C.R. Argoff, G. J. Bennett, M.C. Bushnell, J.T. Farrar, B.S. Galer, J.A. Haythornthwaite, Advances in neuropathic pain: diagnosis, mechanisms, and treatment recommendations, Arch. Neurol. 60 (11) (2003) 1524–1534.
[14] J.H. Vranken, Mechanisms and treatment of neuropathic pain, Cent. Nerv. Syst. Agents Med. Chem. 9 (1) (2009) 71–78.
[15] J. Mao, L.L. Chen, Systemic lidocaine for neuropathic pain relief, Pain 87 (1) (2000) 7–17.
[16] V. Challapalli, I.W. Tremont-Lukats, E.D. McNicol, J. Lau, D.B. Carr, Systemic administration of local anesthetic agents to relieve neuropathic pain, Cochrane Database Syst. Rev. (4) (2005) 1–10.
[17] S. Felsby, J. Nielsen, L. Arendt-Nielsen, T.S. Jensen, NMDA receptor blockade in chronic neuropathic pain: a comparison of ketamine and magnesium chloride, Pain 64 (2) (1996) 283–291.
[18] J. Clements, W. Nimmo, I. Grant, Bioavailability, pharmacokinetics, and analgesic activity of ketamine in humans, J. Pharmaceut. Sci. 71 (5) (1982) 539–542.
[19] J. Malinovsky, F. Servin, A. Cozian, J. Lepage, M. Pinaud, Ketamine and norketamine plasma concentrations after iv, nasal and rectal administration in children, Br. J. Anaesth. 77 (2) (1996) 203–207.
[20] C. Chong, S.A. Schug, M. Page-Sharp, B. Jenkins, K.F. Ilett, Development of a sublingual/oral formulation of ketamine for use in neuropathic pain, Clin. Drug Invest. 29 (5) (2009) 317–324.
[21] B.J. Thomas, B.C. Finnin, The transdermal revolution, Drug Discov. Today 9 (16) (2004) 697–703.
[22] A. Hafeez, U. Jain, J. Singh, A. Maurya, L. Rana, Recent advances in transdermal drug delivery system (TDDS): an overview, J Sci Innov Res 2 (3) (2013) 733–744.
[23] T. Tanner, R. Marks, Delivering drugs by the transdermal route: review and comment, Skin Res. Technol. 14 (3) (2008) 249–260.
[24] K.S. Paudel, M. Milewski, C.L. Swadley, N.K. Brogden, P. Ghosh, A.L. Stinchcomb, Challenges and opportunities in dermal/transdermal delivery, Ther. Deliv. 1 (1) (2010) 109–131.
[25] D.C. Hammell, M. Hamad, H.K. Vaddi, P.A. Crooks, A.L. Stinchcomb, A duplex "Gemini" prodrug of naltrexone for transdermal delivery, J. Contr. Release 97 (2) (2004) 283–290.
[26] N.A. Pescatore, Graphitic Carbon Materials Tailored for the Rapid Adsorption of Biomolecules, Drexel University, 2016.
[27] D. Depan, J. Shah, R. Misra, Controlled release of drug from folate-decorated and graphene mediated drug delivery system: synthesis, loading efficiency, and drug release response, Mater. Sci. Eng. C 31 (7) (2011) 1305–1312.
[28] Q. Zhang, W. Li, T. Kong, R. Su, N. Li, Q. Song, M. Tang, L. Liu, G. Cheng, Tailoring the interlayer interaction between doxorubicin-loaded graphene oxide nanosheets by controlling the drug content, Carbon 51 (2013) 164–172.
[29] M. Zaboli, H. Raissi, N.R. Moghaddam, F. Farzad, Probing the adsorption and release mechanisms of cytarabine anticancer drug on/from dopamine functionalized graphene oxide as a highly efficient drug delivery system, J. Mol. Liq. (2020) 112458.
[30] F. Teodorescu, G. Queniat, C. Foulon, M. Lecoeur, A. Barras, S. Boulahneche, M. S. Medjram, T. Hubert, A. Abderrahmani, R. Boukherroub, Transdermal skin patch based on reduced graphene oxide: a new approach for photothermal triggered permeation of ondansetron across porcine skin, J. Contr. Release 245 (2017) 137–146.
[31] D. Kaya, K. Küçükada, N. Alemdar, Modeling the drug release from reduced graphene oxide-reinforced hyaluronic acid/gelatin/poly (ethylene oxide) polymeric films, Carbohydr. Polym. 215 (2019) 189–197.
[32] A. Pourjavadi, S. Asgari, S.H. Hosseini, Graphene oxide functionalized with oxygen-rich polymers as a pH-sensitive carrier for co-delivery of hydrophobic and hydrophilic drugs, J. Drug Deliv. Sci. Technol. (2020) 101542.
[33] H. Hashemzadeh, H. Raissi, Understanding loading, diffusion and releasing of Doxorubicin and Paclitaxel dual delivery in graphene and graphene oxide carriers as highly efficient drug delivery systems, Appl. Surf. Sci. 500 (2020) 144220.
[34] G. Zapantis, I. Csoka, E. Csanyi, G. Horvath, I. Erős, Evaluation of ketamine systemic absorption from topical preparations, Acta Biol. Hung. 57 (3) (2006) 387–389.
[35] A.S. Bassani, D. Banov, Evaluation of the percutaneous absorption of ketamine HCl, gabapentin, clonidine HCl, and baclofen, in compounded transdermal pain formulations, using the Franz finite dose model, Pain Med. 17 (2) (2016) 230–238.
[36] M. Liu, X. Zheng, Preparation and assessment of ketamine hydrogels for prolonged transdermal anaesthesia, Trop. J. Pharmaceut. Res. 16 (7) (2017) 1481–1487.
[37] R. Kubota, Y. Maruyama, Y. Wada, A. Okamoto, A. Tsukamoto, T. Komiyama, The development of transdermal ketamine patch, Medical Research Archives 6 (4) (2018) 1–9.
[38] B.A. Habib, S. Sayed, G.M. Elsayed, Enhanced transdermal delivery of ondansetron using nanovesicular systems: fabrication, characterization, optimization and ex-vivo permeation study-Box-Cox transformation practical example, Eur. J. Pharmaceut. Sci. 115 (2018) 352–361.
[39] R.M. Al Abood, S. Talegaonkar, M. Tariq, F.J. Ahmad, Microemulsion as a tool for the transdermal delivery of ondansetron for the treatment of chemotherapy induced nausea and vomiting, Colloids Surf. B Biointerfaces 101 (2013) 143–151.
[40] B. Paulchamy, G. Arthi, B. Lignesh, A simple approach to stepwise synthesis of graphene oxide nanomaterial, Nanomed Nanotechnol 6 (1) (2015) 1–12.
[41] N. Zaaba, K. Foo, U. Hashim, S. Tan, W.-W. Liu, C. Voon, Synthesis of graphene oxide using modified hummers method: solvent influence, Procedia engineering 184 (2017) 469–477.
[42] R. Cherian, S. Sandeman, S. Ray, I. Savina, J. Ashtami, P. Mohanan, Green synthesis of Pluronic stabilized reduced graphene oxide: chemical and biological characterization, Colloids Surf. B Biointerfaces 179 (2019) 94–106.
[43] N.S. Andryushina, O.L. Stroyuk, I.B. Yanchuk, A.V. Yefanov, A dynamic light scattering study of photochemically reduced colloidal graphene oxide, Colloid Polym. Sci. 292 (2) (2014) 539–546.
[44] X. Hu, Y. Yu, W. Hou, J. Zhou, L. Song, Effects of particle size and pH value on the hydrophilicity of graphene oxide, Appl. Surf. Sci. 273 (2013) 118–121.
[45] F.A. Maulvi, R.J. Patil, A.R. Desai, M.R. Shukla, R.J. Vaidya, K.M. Ranch, B. A. Vyas, S.A. Shah, D.O. Shah, Effect of gold nanoparticles on timolol uptake and its release kinetics from contact lenses: in vitro and in vivo evaluation, Acta Biomater. 86 (2019) 350–362.
[46] G. Wang, X. Shen, B. Wang, J. Yao, J. Park, Synthesis and characterisation of hydrophilic and organophilic graphene nanosheets, Carbon 47 (5) (2009) 1359–1364.
[47] M. Yadav, K.Y. Rhee, S. Park, Synthesis and characterization of graphene oxide/carboxymethylcellulose/alginate composite blend films, Carbohydr. Polym. 110 (2014) 18–25.
[48] A. Kaniyoor, S.J.A.A. Ramaprabhu, A Raman spectroscopic investigation of graphite oxide derived graphene 2 (3) (2012), 032183.
[49] D. Yang, A. Velamakanni, G. Bozoklu, S. Park, M. Stoller, R.D. Piner, S. Stankovich, I. Jung, D.A. Field, C.A. Ventrice Jr., Chemical analysis of graphene oxide films

after heat and chemical treatments by X-ray photoelectron and Micro-Raman spectroscopy, Carbon 47 (1) (2009) 145–152.
[50] I. Childres, L.A. Jauregui, W. Park, H. Cao, Y.P. Chen, Raman spectroscopy of graphene and related materials, New developments in photon materials research 1 (2013) 1–20.
[51] L. Stobinski, B. Lesiak, A. Malolepszy, M. Mazurkiewicz, B. Mierzwa, J. Zemek, P. Jiricek, I. Bieloshapka, Graphene oxide and reduced graphene oxide studied by the XRD, TEM and electron spectroscopy methods, J. Electron. Spectrosc. Relat. Phenom. 195 (2014) 145–154.
[52] A. Shalaby, D. Nihtianova, P. Markov, A. Staneva, R. Iordanova, Y. Dimitriev, Structural analysis of reduced graphene oxide by transmission electron microscopy, Bulgarian Chemical Communications 47 (1) (2015) 291–295.
[53] J. Wan, F. Shen, W. Luo, L. Zhou, J. Dai, X. Han, W. Bao, Y. Xu, J. Panagiotopoulos, X. Fan, In situ transmission electron microscopy observation of sodiation–desodiation in a long cycle, high-capacity reduced graphene oxide sodium-ion battery anode, Chem. Mater. 28 (18) (2016) 6528–6535.
[54] S. Pandey, S.V. Swamy, A. Gupta, A. Koli, S. Patel, F. Maulvi, B. Vyas, Multiple response optimisation of processing and formulation parameters of pH sensitive sustained release pellets of capecitabine for targeting colon, J. Microencapsul. 35 (3) (2018) 259–271.
[55] A. Ahad, M. Aqil, A. Ali, Investigation of antihypertensive activity of carbopol valsartan transdermal gel containing 1, 8-cineole, Int. J. Biol. Macromol. 64 (2014) 144–149.
[56] F.A. Maulvi, L.V. Pillai, K.P. Patel, A.R. Desai, M.R. Shukla, D.T. Desai, H.P. Patel, K.M. Ranch, S.A. Shah, D.O. Shah, Lidocaine tripotassium phosphate complex laden microemulsion for prolonged local anaesthesia: in vitro and in vivo studies, Colloids Surf. B Biointerfaces 185 (2020) 110632.
[57] S.S. Pandey, F.A. Maulvi, P.S. Patel, M.R. Shukla, K.M. Shah, A.R. Gupta, S. V. Joshi, D.O. Shah, Cyclosporine laden tailored microemulsion-gel depot for effective treatment of psoriasis: in vitro and in vivo studies, Colloids Surf. B Biointerfaces 186 (2020) 110681.
[58] S.S. Pandey, M.A. Patel, D.T. Desai, H.P. Patel, A.R. Gupta, S.V. Joshi, D.O. Shah, F. A. Maulvi, Bioavailability enhancement of repaglinide from transdermally applied nanostructured lipid carrier gel: optimization, in vitro and in vivo studies, J. Drug Deliv. Sci. Technol. (2020) 101731.
[59] H. Adams, B. Weber, B. Bachmann-M, M. Guerin, G. Hempelmann, The simultaneous determination of ketamine and midazolam using high pressure liquid chromatography and UV detection (HPLC/UV), Anaesthesist 41 (10) (1992) 619–624.
[60] A. Gross, A. Nicolay, A. Eschalier, Simultaneous analysis of ketamine and bupivacaine in plasma by high-performance liquid chromatography, J. Chromatogr. B Biomed. Sci. Appl. 728 (1) (1999) 107–115.
[61] O. Pillai, R. Panchagnula, Transdermal delivery of insulin from poloxamer gel: ex vivo and in vivo skin permeation studies in rat using iontophoresis and chemical enhancers, J. Contr. Release 89 (1) (2003) 127–140.
[62] J. Hurkmans, H. Bodde, L. Van Driel, H. Van Doorne, H. Junginger, Skin irritation caused by transdermal drug delivery systems during long-term (5 days) application, Br. J. Dermatol. 112 (4) (1985) 461–467.
[63] F.A. Maulvi, V.T. Thakkar, T.G. Soni, T.R. Gandhi, Optimization of aceclofenac solid dispersion using Box-Behnken design: in-vitro and in-vivo evaluation, Curr. Drug Deliv. 11 (3) (2014) 380–391.
[64] P.R. Dash, M. Nasrin, M.T.I. Morshed, M.S. Ali, Study of antinociceptive activity of Kaempferia galanga from Bangladesh in Swiss albino mice, American Journal of Food Nutrition 3 (3) (2015) 64–68.
[65] G. Sharma, S. Kamboj, K. Thakur, P. Negi, K. Raza, O. Katare, Delivery of thermoresponsive-tailored mixed micellar nanogel of lidocaine and prilocaine with improved dermatokinetic profile and therapeutic efficacy in topical anaesthesia, AAPS PharmSciTech 18 (3) (2017) 790–802.
[66] O.-G. Berge, I. Garcia-Cabrera, K. Hole, Response latencies in the tail-flick test depend on tail skin temperature, Neurosci. Lett. 86 (3) (1988) 284–288.
[67] A. Dogrul, S.E. Gülmez, M.S. Deveci, H. Gul, M.H. Ossipov, F. Porreca, F. C. Tulunay, The local antinociceptive actions of nonsteroidal antiinflammatory drugs in the mouse radiant heat tail-flick test, Anesth. Analg. 104 (4) (2007) 927–935.
[68] J. Parra, M. Paye, EEMCO guidance for the in vivo assessment of skin surface pH, Skin Pharmacol. Physiol. 16 (3) (2003) 188–202.
[69] D. Ma, J. Lin, Y. Chen, W. Xue, L.-M. Zhang, In situ gelation and sustained release of an antitumor drug by graphene oxide nanosheets, Carbon 50 (8) (2012) 3001–3007.
[70] F. Barahuie, B. Saifullah, D. Dorniani, S. Fakurazi, G. Karthivashan, M.Z. Hussein, F.M. Elfghi, Graphene oxide as a nanocarrier for controlled release and targeted delivery of an anticancer active agent, chlorogenic acid, Mater. Sci. Eng. C 74 (2017) 177–185.
[71] D. Sibalis, Transdermal Drug Delivery System, Google Patents, 1992.
[72] R.H. Kronenberg, Ketamine as an analgesic: parenteral, oral, rectal, subcutaneous, transdermal and intranasal administration, J. Pain Palliat. Care Pharmacother. 16 (3) (2002) 27–35.